Physical constraints for effective magma-water interaction along volcanic conduits during silicic explosive eruptions

Alvaro Aravena[1], Mattia de' Michieli Vitturi[2], Raffaello Cioni[1] and Augusto Neri[2]

[1]*Dipartimento di Scienze della Terra, Università di Firenze, 50121 Florence, Italy*

[2]*Istituto Nazionale di Geofisica e Vulcanologia, Sezione di Pisa, 56126 Pisa, Italy*

ABSTRACT

The entry of groundwater into volcanic conduits has been proposed as a major modifying agent of eruptive dynamics, influencing magma fragmentation and pyroclast dispersion. Although several external water sources and interaction mechanisms have been proposed, the nature and effects of magma-water interaction are still largely unclear, as well as its controlling factors. A common postulate for phreatomagmatic activity to occur is that pressure in a conduit crosscutting a subsurface aquifer should drop below the aquifer pressure, which depends on the properties of the aquifer and ascending magma. In agreement with most phreatomagmatic eruptions, we show that the injection of large mass fractions of groundwater during silicic explosive eruptions (e.g., >5 wt%) is only physically feasible for low-eruption-rate events; while high-intensity eruptions with evidence of magma-water interaction are probably related to other interaction mechanisms (e.g., the involvement of surface water or the destabilization of aquifer-hosting rocks during collapse phases). Because conditions for access of groundwater to the conduit are preferably reached above the fragmentation level, magma-water interaction seems not to induce dramatic changes to the features of a primary 'dry' vesicularity, as commonly claimed. Hence, the low vesicularity indexes often attributed to phreatomagmatic eruptions

appear difficult to explain by the quenching effect of groundwater on a not-fully developed vesicularity. Instead, they may be related to the low eruption rates needed for effective magma-water interaction, generally characterized by significant lateral gradients of vesicularity in narrow conduits.

INTRODUCTION

Magma-water interaction appears able to produce significant changes in the behavior of explosive eruptions, manifested in modifications in the fragmentation dynamics, transport, and deposition mechanisms (Sheridan and Wohletz, 1983; Lorenz, 1987; Pedrazzi et al., 2014). Several studies have addressed the interaction dynamics between magma and external water (e.g., White, 1996), suggesting the main processes that external water injection involves: fuel-coolant interaction and magma quenching. The mass ratio between water and melt controls the interaction dynamics, and an optimal water mass fraction has been estimated for the maximum conversion of thermal energy into mechanical energy, set between 0.1 and 0.3 (Sheridan and Wohletz, 1983; Wohletz, 1986). Hence, the amount of water that effectively can be injected into volcanic conduits is a key topic to assess the occurrence of hydromagmatic eruptions, and we consider that the mechanisms leading to magma-water interaction are still largely unknown. Sources of external water can be split into surface and groundwater. While vent location is the main controlling factor for the entry of surface water, groundwater injection can only occur when magma pressure in the conduit drops below the aquifer pressure (Barberi et al., 1989), and thus it is controlled by the interplay between the conduit and the hydrologic system (Starostin et al., 2005). In this work, we study the conditions required to inject significant volumes of groundwater into volcanic conduits during silicic explosive events, providing for the first

time important constraints of the conditions needed to produce phreatomagmatic eruptions, their effects on eruptive dynamics, and the relationship between phreatomagmatic interaction and the vesicularity index of pyroclasts (Houghton and Wilson, 1989). These constraints are fundamental to define the limiting conditions for the development of significant magma-water interaction and phreatomagmatic eruptions. In particular, we consider trachytic, dacitic, and rhyolitic magmas because of their importance for phreatomagmatic volcanism (Heiken and Wohletz, 1987; Orsi et al., 1992; Cole et al., 1995), while basaltic melts were not addressed in this work. The term 'phreatomagmatic' has been employed in many different ways in volcanology (e.g., Barberi et al., 1989; White, 1996). Following Liu et al. (2017), we use the term 'phreatomagmatic' specifically for referring to interaction between magma and groundwater.

METHODS

For this investigation, we used the code MAMMA (Magma Ascent Mathematical Modeling and Analysis), which is an updated version of the steady-state model of volcanic conduit dynamics presented by de' Michieli Vitturi et al. (2011) and La Spina et al. (2015). The code considers the main processes experienced by magmas during ascent through a vertical conduit (see the GSA Data Repository[1] for the system of equations). Because the groundwater injection is modeled using Darcy's Law, it is controlled by aquifer properties and the magma pressure profile. Aquifers are characterized by permeability (k), depth, thickness, and pressure profile, and two natural end-members are considered here: normally pressured aquifers (hydrostatic pressure gradient), and geopressured aquifers (lithostatic pressure gradient). For each end-member, we performed a set of simulations using variable values for inlet pressure, water content at the conduit bottom, conduit radius,

aquifer depth (500–2000 m), and thickness (150–300 m), considering a 5000-m-long cylindrical conduit and a temperature at conduit bottom of 900 °C (further information is presented in the Data Repository). We model different aquifer permeabilities between 10^{-11} and 10^{-14} m^2, thus including representative values for natural conditions (Reid, 2004; Sruoga et al., 2004). The model outputs are the profiles along the conduit of relevant physical parameters of the magma (e.g., pressure and temperature). Output data analysis was split into three parts. First, we studied the conditions that favor the injection of significant amounts of groundwater, quantified as the ratio between external water flux and mass discharge rate (MDR). Second, in order to evaluate conduit mechanical stability, we used the model described by Aravena et al. (2017). Finally, we studied the effects of groundwater on the ascending magma by comparing relevant eruptive parameters of the modeled phreatomagmatic events versus simulations with no aquifer. Given that trachytic melts result in the most favorable conditions for magma-water interaction to occur, we mainly refer to this composition in the following sections. Results associated to other compositions are consistent with these magmas, and are shown in the Data Repository.

RESULTS

Favorable Conditions for Magma-Water Interaction

Because the pressure profile in the conduit is controlled by the fragmentation depth, the relative location between the aquifer and fragmentation level determines the behavior of the system. It is therefore convenient to analyze the results according to this relative position. For aquifers located above the fragmentation level (Fig. 1A; regime 1 of Starostin et al. [2005]), the injection of groundwater produces a significant effect on pressure and velocity profiles of ascending magma. In this case, in order to satisfy the exit condition

92 (i.e., atmospheric pressure, or choked flow), the model predicts that the fragmentation level
93 stabilizes at a shallower position with respect to the case with no aquifer. Because of the
94 large pressure drop near the fragmentation level, the injection of water above magma
95 fragmentation occurs for a wide range of input parameters. Figure 1B illustrates the case
96 in which the aquifer is located at the same depth as the fragmentation level (regime 2). In
97 this case, the water inflow induces a significant change in the pressure profile and a slightly
98 deeper fragmentation level than that observed for simulations with no aquifer. Finally,
99 Figure 1C shows a typical case in which the aquifer is located below the fragmentation
100 level (regime 3). Because conduit pressure below magma fragmentation is close to the
101 lithostatic pressure, water injection occurs almost exclusively when geopressured aquifers
102 are considered. In this case, the fragmentation level is drastically deepened by the presence
103 of the aquifer.

104 The mass of external water entering the conduit is strongly affected by the aquifer's
105 physical parameters (Figs. 2 and 3; Figs. DR7–DR10 in the Data Repository), and high
106 proportions of injected water are only possible for highly permeable aquifers. Indeed, for
107 dacitic and trachytic magmas, relative amounts of up to 15–30 wt% of the resulting erupted
108 mixture for normally pressured aquifers and up to 40–50 wt% in case of geopressured
109 aquifers, are reached only for $k = 10^{-11}$ m^2. Importantly, such high water/magma ratios
110 were obtained only for the lowest MDRs derived from this study, corresponding to values
111 lower than 3×10^6 and 10^6 kg/s for dacitic and trachytic magmas, respectively. In contrast,
112 rhyolitic magmas and/or low-permeability aquifers ($k < 10^{-12}$ m^2) do not seem able to
113 induce the injection of significant mass fractions of groundwater, even for geopressured
114 aquifers. Moreover, it is worth noting that aquifer pressurization can result in low-

permeability conditions, and thus the occurrence of geopressured, high-permeability aquifers can be naturally hindered (Hart et al., 1995). Hence, the conditions needed to produce phreatomagmatic events are even more restricted in nature when geopressured aquifers are considered.

Significant ratios of injected water (here assumed corresponding to >5 wt% of the erupted mixture) are only achieved for narrow conduits and low MDRs. Specifically, significant mass fractions of external water are limited to MDR < 4×10^6 kg/s and MDR < 10^7 kg/s for trachytic magmas with normally pressured and geopressured aquifers, respectively (considering $k = 10^{-11}$ m^2); and MDR < 10^7 kg/s and MDR < 2×10^7 for dacitic magmas with normally pressured and geopressured aquifers, respectively (considering $k = 10^{-11}$ m^2); while these mass fractions of groundwater are never reached for permeabilities lower than 10^{-12} m^2 (Figs. 2 and 3; Figs. DR7–DR10). It emerges that, although wide conduits present larger injection surfaces, the associated events are characterized by higher MDRs, and external water fluxes are not large enough to inject a significant part of the resulting erupted mixture. Indeed, the high MDR typical of explosive rhyolitic eruptions hinders the occurrence of significant magma-water interaction in these events (Figs. DR9 and DR10).

Effects of Groundwater on the Ascending Magma

The injection of significant quantities of groundwater is almost exclusively observed when the aquifer is located above the fragmentation level (Figs. 2 and 3); otherwise, the injected water mass fraction rarely exceeds 1 wt%. In the few cases in which groundwater injection occurs below the fragmentation level, magma-water interaction is still expected to occur with highly-vesicular melts (>60 vol% of bubbles, or so). Depending

on the relative position between magma fragmentation and aquifer, the groundwater inflow may cause significant changes to key eruptive parameters (Fig. 4), which is in agreement with Starostin et al. (2005). In particular, when groundwater injection occurs above magma fragmentation, it produces an increase in MDR. This is a consequence of the addition of kinetic energy derived from the expanding injected material, which trigger an adjustment of the pressure profile to satisfy the exit condition, deepening the fragmentation level and increasing the MDR. In contrast, the interaction between groundwater and non-fragmented magma does not necessarily induce fragmentation conditions, and so can cause a cooling-driven increase of magma viscosity, reducing the ascent rate and producing less intense volcanic events. Also, the injection of significant amounts of external water appears able to substantially decrease the eruption temperature (e.g., 10 wt% of external water is able to reduce the eruption temperature by 100 °C; Fig. 4) and increase the exit pressure and velocity (e.g., 10 wt% of added groundwater can lead to increases of 50%–100% in exit velocity and 50%–200% in exit pressure; Fig. 4), with major consequences on the regime of the volcanic column (Neri and Dobran, 1994; Colucci et al., 2014). Conversely, the low amounts of groundwater expected for MDRs higher than 10^7 kg/s (i.e., Plinian and most sub-Plinian events; Cioni et al., 2015) result in weak changes of eruptive parameters and thus they are poorly recorded in pyroclastic deposits.

VOLCANOLOGICAL IMPLICATIONS

The fact that the injection of significant mass fractions of groundwater is limited to low-intensity events could explain why phreatomagmatic activity is commonly related to eruptions of low MDR (e.g., Cole et al., 1995), often associated to the formation of tuff rings (e.g., Heiken and Wohletz, 1987). In contrast, we suggest that events with high MDR

and evidence for magma-water interaction are probably related to other interaction mechanisms, such as the involvement of surface water or the injection of groundwater by high-magnitude collapse mechanisms (e.g., crater- or caldera-forming events; Cioni et al., 1999; Sulpizio et al., 2010). For instance, events of particularly high intensity described as phreato-Plinian eruptions such as some of those generated by Taupo (New Zealand) or Askja (Iceland) volcanoes, or Campi Flegrei (Italy) caldera (Sparks et al., 1981; Walker, 1981; Orsi et al., 1992), can only be explained with the involvement of surface water in the eruptive dynamics. Conversely, magma-water interaction during high intensity events repeatedly occurred at Vesuvius, Italy (Cioni et al., 1999; Sulpizio et al., 2010) and other volcanoes (e.g., the Minoan eruption of Santorini, Greece; Heiken and McCoy, 1984), but they always coincided with phases of caldera collapse. This well agrees with our results, which show that natural aquifers appear unlikely to be sources of enough water to significantly affect the eruptive dynamics of such intense events (thus, we would better term these events as "hydro-Plinian eruptions").

The opening phases of volcanic eruptions (i.e., characterized by narrow conduits with high ratios between water injection surface and cross section area) present favorable conditions to produce magma-water interaction, as observed in several case studies (Cioni et al., 2000; Houghton et al., 2004). Since the presence of aquifers can destabilize the volcanic conduit due to the pore pressure influence on conduit mechanical stability (Aravena, 2017), these opening phreatomagmatic phases may represent an effective mechanism for early widening of volcanic conduits. Moreover, favorable conditions for external water injection are characterized by mechanically unstable conduits (Fig. DR11), and thus the occurrence of collapse processes is favored. Hence, phreatomagmatic

184 interaction would be commonly related to the emission of relatively high volumes of lithic
185 fragments, as described in many study cases (Barberi et al., 1989; Cole et al., 1995).
186 Phreatomagmatic eruptions have been traditionally related to low vesicularity
187 indexes (<40%) and broad vesicularity ranges (up to 80%) in the pyroclastic products
188 (Houghton and Wilson, 1989), commonly explained as the effect of magma quenching
189 before reaching conditions of 'dry' fragmentation. 'Dry' fragmentation in high MDR
190 events is expected to produce high vesicularity indexes (>70%–80%) and narrow
191 vesicularity ranges (<25%), whereas 'dry' fragmentation in low eruption rate events is
192 often related to the production of fragments with a largely variable vesicularity (Houghton
193 and Wilson, 1989). Because the entry of significant fractions of external water is almost
194 exclusively observed above the fragmentation level, results suggest that magma-water
195 interaction along the conduit should not produce an important modification of pyroclast
196 vesicularity, which would instead record the primary vesiculation conditions. For example,
197 relatively low vesicularity indexes (<60%) and broad vesicularity ranges (up to 80%), in
198 the absence of clear evidences of the involvement of external water, have been reported for
199 the 'dry' sub-Plinian greenish pumice eruption of Somma-Vesuvius (MDR~$2 \cdot 10^7$ kg/s)
200 (Cioni et al., 2003). In this case, the presence of dense juvenile fragments in such a low
201 eruption rate event has been explained by significant lateral gradients in the ascending
202 magma, degassing processes and groundmass crystallization (Cioni et al., 2003). Hence,
203 results suggest that low vesicularity indexes and broad vesicularity ranges are not
204 necessarily related to magma-water interaction; and additional evidence should be
205 employed for proposing the involvement of external water in explosive events (White and
206 Valentine, 2016). More likely, the effects of groundwater could be limited to other eruption

features, such as grain-size distribution of pyroclasts, water content of groundmass glass, deposition mechanisms and eruptive parameters.

REFERENCES CITED

Aravena, A., 2017, Stability of volcanic conduits: Critical mechanical parameters: Il Nuovo Cimento, v. 40, no. 96, https://doi.org/10.1393/ncc/i2017-17096-3.

Aravena, A., de' Michieli Vitturi, M., Cioni, R., and Neri, A., 2017, Stability of volcanic conduits during explosive eruptions: Journal of Volcanology and Geothermal Research, v. 339, p. 52–62, https://doi.org/10.1016/j.jvolgeores.2017.05.003.

Barberi, F., Cioni, R., Rosi, M., Santacroce, R., Sbrana, A., and Vecci, R., 1989, Magmatic and phreatomagmatic phases in explosive eruptions of Vesuvius as deduced by grain-size and component analysis of the pyroclastic deposits: Journal of Volcanology and Geothermal Research, v. 38, p. 287–307, https://doi.org/10.1016/0377-0273(89)90044-9.

Cioni, R., Santacroce, R., and Sbrana, A., 1999, Pyroclastic deposits as a guide for reconstructing the multi-stage evolution of the Somma-Vesuvius Caldera: Bulletin of Volcanology, v. 61, p. 207–222, https://doi.org/10.1007/s004450050272.

Cioni, R., Gurioli, L., Sbrana, A., and Vougioukalakis, G., 2000, Precursory phenomena and destructive events related to the Late Bronze Age Minoan (Thera, Greece) and AD 79 (Vesuvius, Italy) Plinian eruptions; Inferences from the stratigraphy in the archaeological areas, *in* McGuire, W.J., et al., eds., The Archaeology of Geological Catastrophes: Geological Society of London Special Publications, v. 171, p. 123–141, https://doi.org/10.1144/GSL.SP.2000.171.01.11.

Cioni, R., Sulpizio, R., and Garruccio, N., 2003, Variability of the eruption dynamics during a subplinian event: The Greenish Pumice eruption of Somma–Vesuvius (Italy): Journal of Volcanology and Geothermal Research, v. 124, p. 89–114, https://doi.org/10.1016/S0377-0273(03)00070-2.

Cioni, R., Pistolesi, M., and Rosi, M., 2015, Plinian and Subplinian eruptions: The Encyclopedia of Volcanoes (Second Edition): Elsevier, p. 519–535, https://doi.org/10.1016/B978-0-12-385938-9.00029-8.

Cole, P., Queiroz, G., Wallenstein, N., Gaspar, J., Duncan, A., and Guest, J., 1995, An historic subplinian/phreatomagmatic eruption: the 1630 AD eruption of Furnas volcano, Sao Miguel, Azores: Journal of Volcanology and Geothermal Research, v. 69, p. 117–135, https://doi.org/10.1016/0377-0273(95)00033-X.

Colucci, S., de' Michieli Vitturi, M., Neri, A., and Palladino, D., 2014, An integrated model of magma chamber, conduit, and column for the analysis of sustained magmatic eruptions: Earth and Planetary Science Letters, v. 404, p. 98–110, https://doi.org/10.1016/j.epsl.2014.07.034.

De' Michieli Vitturi, M., Clarke, A., Neri, A., and Voight, B., 2011, Assessing the influence of disequilibrium crystallization and degassing during magma ascent in effusive and explosive eruptions: Proceedings American Geophysical Union Fall Meeting Abstracts 2011, v. 1, p. 05.

Hart, B., Flemings, P., and Deshpande, A., 1995, Porosity and pressure: Role of compaction disequilibrium in the development of geopressures in a Gulf Coast Pleistocene basin: Geology, v. 23, p. 45–48, https://doi.org/10.1130/0091-7613(1995)023<0045:PAPROC>2.3.CO;2.

252 Heiken, G., and McCoy, F., 1984, Caldera development during the Minoan eruption, Thira,
253 Cyclades, Greece: Journal of Geophysical Research: Solid Earth, v. 89, B10, p. 8441–
254 8462, https://doi.org/10.1029/JB089iB10p08441.
255 Heiken, G., and Wohletz, K., 1987, Tephra deposits associated with silicic domes and lava
256 flows, *in* Fink, J.H., ed., The Emplacement of Silicic Domes and Lava Flows:
257 Geological Society of America Special Papers, v. 212, p. 55–76,
258 https://doi.org/10.1130/SPE212-p55.
259 Houghton, B., and Wilson, C., 1989, A vesicularity index for pyroclastic deposits: Bulletin
260 of Volcanology, v. 51, p. 451–462, https://doi.org/10.1007/BF01078811.
261 Houghton, B., Wilson, C., Del Carlo, P., Coltelli, M., Sable, J., and Carey, R., 2004, The
262 influence of conduit processes on changes in style of basaltic Plinian eruptions:
263 Tarawera 1886 and Etna 122 BC: Journal of Volcanology and Geothermal Research,
264 v. 137, p. 1–14, https://doi.org/10.1016/j.jvolgeores.2004.05.009.
265 La Spina, G., Burton, M., and de' Michieli Vitturi, M., 2015, Temperature evolution during
266 magma ascent in basaltic effusive eruptions: A numerical application to Stromboli
267 volcano: Earth and Planetary Science Letters, v. 426, p. 89–100,
268 https://doi.org/10.1016/j.epsl.2015.06.015.
269 Liu, E.J., Cashman, K., Rust, A., and Höskuldsson, A., 2017, Contrasting mechanisms of
270 magma fragmentation during coeval magmatic and hydromagmatic activity: The
271 Hverfjall Fires fissure eruption, Iceland: Bulletin of Volcanology, v. 79, p. 68,
272 https://doi.org/10.1007/s00445-017-1150-8.
273 Lorenz, V., 1987, Phreatomagmatism and its relevance: Chemical Geology, v. 62, p. 149–
274 156, https://doi.org/10.1016/0009-2541(87)90066-0.

Neri, A., and Dobran, F., 1994, Influence of eruption parameters on the thermofluid dynamics of collapsing volcanic columns: Journal of Geophysical Research: Solid Earth, v. 99, B6, p. 11833–11857, https://doi.org/10.1029/94JB00471.

Orsi, G., D'Antonio, M., de Vita, S., and Gallo, G., 1992, The Neapolitan Yellow Tuff, a large-magnitude trachytic phreatoplinian eruption: eruptive dynamics, magma withdrawal and caldera collapse: Journal of Volcanology and Geothermal Research, v. 53, p. 275–287, https://doi.org/10.1016/0377-0273(92)90086-S.

Pedrazzi, D., Bolós, X., and Martí, J., 2014, Phreatomagmatic volcanism in complex hydrogeological environments: La crosa de Sant Dalmai maar (Catalan Volcanic Zone, NE Spain): Geosphere, v. 10, p. 170–184, https://doi.org/10.1130/GES00959.1.

Reid, M.E., 2004, Massive collapse of volcano edifices triggered by hydrothermal pressurization: Geology, v. 32, p. 373–376, https://doi.org/10.1130/G20300.1.

Sheridan, M.F., and Wohletz, K.H., 1983, Hydrovolcanism: basic considerations and review: Journal of Volcanology and Geothermal Research, v. 17, p. 1–29, https://doi.org/10.1016/0377-0273(83)90060-4.

Sparks, R.S.J., Wilson, L., and Sigurdsson, H., 1981, The pyroclastic deposits of the 1875 eruption of Askja, Iceland: Philosophical Transactions of the Royal Society of London: Series A, Mathematical and Physical Sciences, v. 299, p. 241–273, https://doi.org/10.1098/rsta.1981.0023.

Sruoga, P., Rubinstein, N., and Hinterwimmer, G., 2004, Porosity and permeability in volcanic rocks: A case study on the Serie Tobífera, South Patagonia, Argentina: Journal of Volcanology and Geothermal Research, v. 132, p. 31–43, https://doi.org/10.1016/S0377-0273(03)00419-0.

298 Starostin, A., Barmin, A., and Melnik, O., 2005, A transient model for explosive and
299 phreatomagmatic eruptions: Journal of Volcanology and Geothermal Research,
300 v. 143, p. 133–151, https://doi.org/10.1016/j.jvolgeores.2004.09.014.
301 Sulpizio, R., Cioni, R., Di Vito, M.A., Mele, D., Bonasia, R., and Dellino, P., 2010, The
302 Pomici di Avellino eruption of Somma-Vesuvius (3.9 ka BP). Part I: Stratigraphy,
303 compositional variability and eruptive dynamics: Bulletin of Volcanology, v. 72,
304 p. 539–558, https://doi.org/10.1007/s00445-009-0339-x.
305 Walker, G.P., 1981, Characteristics of two phreatoplinian ashes, and their water-flushed
306 origin: Journal of Volcanology and Geothermal Research, v. 9, p. 395–407,
307 https://doi.org/10.1016/0377-0273(81)90046-9.
308 White, J.D., 1996, Impure coolants and interaction dynamics of phreatomagmatic
309 eruptions: Journal of Volcanology and Geothermal Research, v. 74, p. 155–170,
310 https://doi.org/10.1016/S0377-0273(96)00061-3.
311 White, J.D., and Valentine, G.A., 2016, Magmatic versus phreatomagmatic fragmentation:
312 Absence of evidence is not evidence of absence: Geosphere, v. 12, p. 1478–1488,
313 https://doi.org/10.1130/GES01337.1.
314 Wohletz, K.H., 1986, Explosive magma-water interactions: Thermodynamics, explosion
315 mechanisms, and field studies: Bulletin of Volcanology, v. 48, p. 245–264,
316 https://doi.org/10.1007/BF01081754.
317

FIGURE CAPTIONS

Figure 1. Pressure profiles for a specific set of simulations (water content at conduit bottom: 6.0 wt%; inlet overpressure: −10 MPa; conduit radius: 15 m; aquifer permeability: 10^{-11} m^2). A: Representative case of simulations with the aquifer located above the fragmentation level. B: Representative case of simulations with the fragmentation level located within the aquifer. C: Representative case of simulations with the aquifer located below the fragmentation level. Figures DR1–DR6 (see footnote 1) present the profiles along the conduit of additional variables for representative simulations of the described regimes.

Figure 2. Injected water mass fraction versus mass discharge rate, as a function of aquifer permeability and the relative position between aquifer and magma fragmentation, considering normally pressured aquifers and trachytic magmas. The results associated with dacitic and rhyolitic magmas are presented in Figures DR7–DR10 (see footnote 1).

Figure 3. Injected water mass fraction versus mass discharge rate, as a function of aquifer permeability and the relative position between aquifer and magma fragmentation, considering geopressured aquifers and trachytic magmas. The results associated with dacitic and rhyolitic magmas are presented in Figures DR7–DR10 (see footnote 1).

Figure 4. Comparison between resulting eruptive dynamics of phreatomagmatic eruptions and the equivalent simulations with no aquifer (i.e., using the same values for water content at the conduit bottom, inlet pressure, and conduit radius), as a function of the mass fraction

of groundwater entered into the conduit. A: Ratio of mass discharge rates. B: Ratio of exit velocities. C: Ratio of exit pressures. D: Decrease of exit temperature.

Figure 1

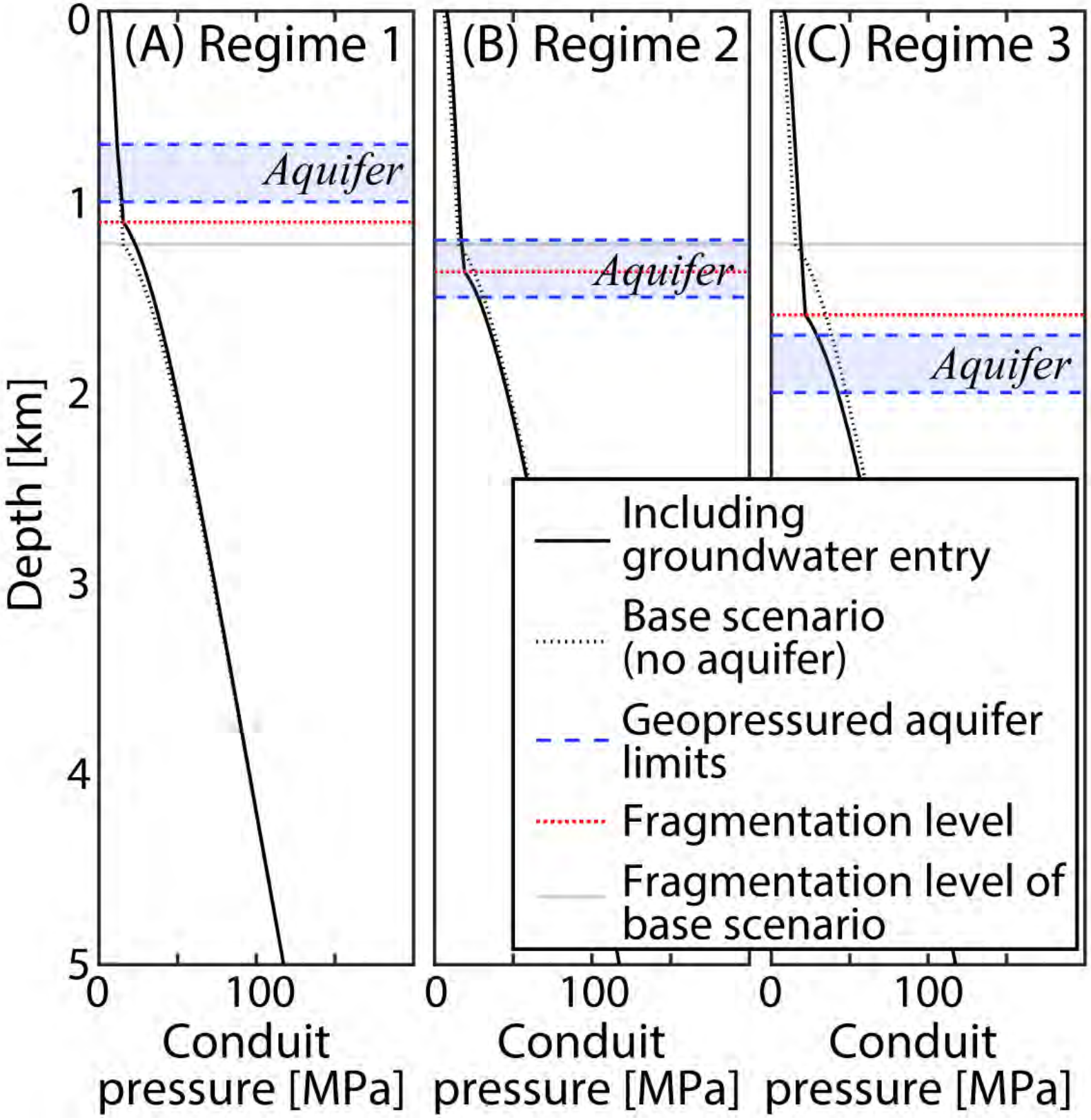
(A) Regime 1
(B) Regime 2
(C) Regime 3
Aquifer
Aquifer
Aquifer
Depth [km]
0
1
2
3
4
5
0
100
Conduit pressure [MPa]
Including groundwater entry
Base scenario (no aquifer)
Geopressured aquifer limits
Fragmentation level
Fragmentation level of base scenario

Figure 2

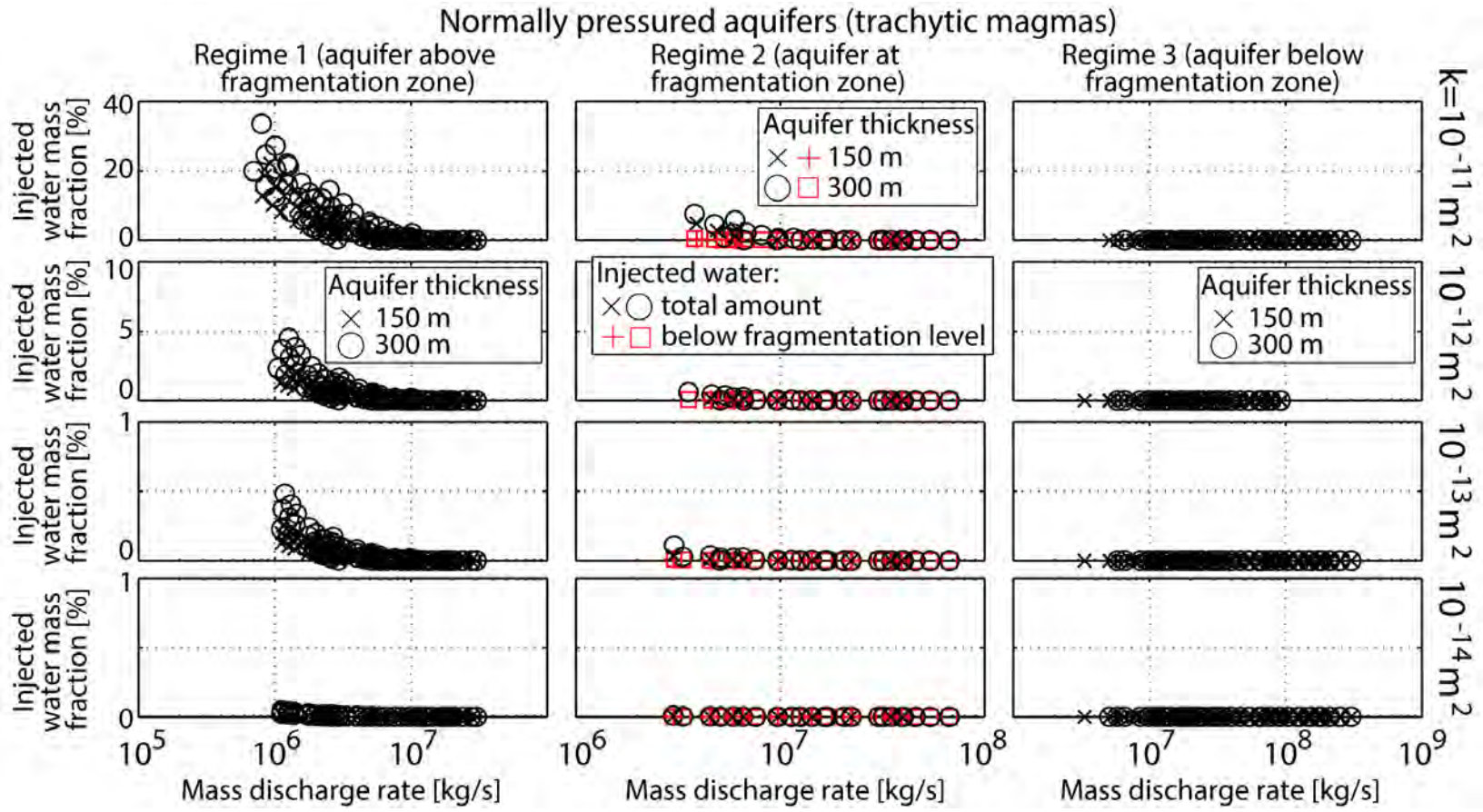
Normally pressured aquifers (trachytic magmas)
Regime 1 (aquifer above fragmentation zone)
Regime 2 (aquifer at fragmentation zone)
Regime 3 (aquifer below fragmentation zone)
Injected water mass fraction [%]
Aquifer thickness
150 m
300 m
Injected water:
total amount
below fragmentation level
k=10^-11 m^2
k=10^-12 m^2
k=10^-13 m^2
k=10^-14 m^2
Mass discharge rate [kg/s]

Figure 3

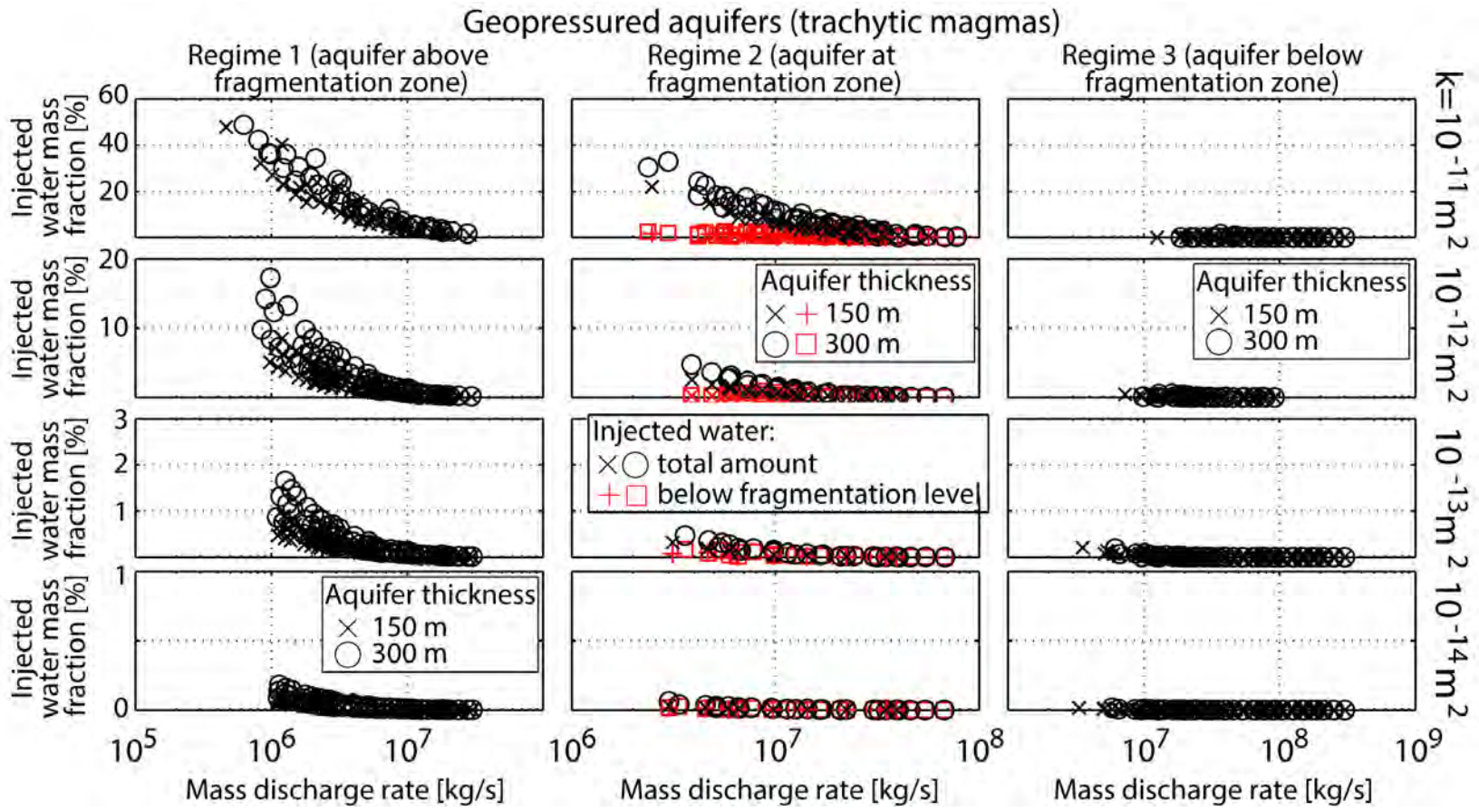
Geopressured aquifers (trachytic magmas)
Regime 1 (aquifer above fragmentation zone)
Regime 2 (aquifer at fragmentation zone)
Regime 3 (aquifer below fragmentation zone)
k=10^-11 m^2
10^-12 m^2
10^-13 m^2
10^-14 m^2
Injected water mass fraction [%]
Aquifer thickness
150 m
300 m
Injected water:
total amount
below fragmentation level
Mass discharge rate [kg/s]

Figure 4

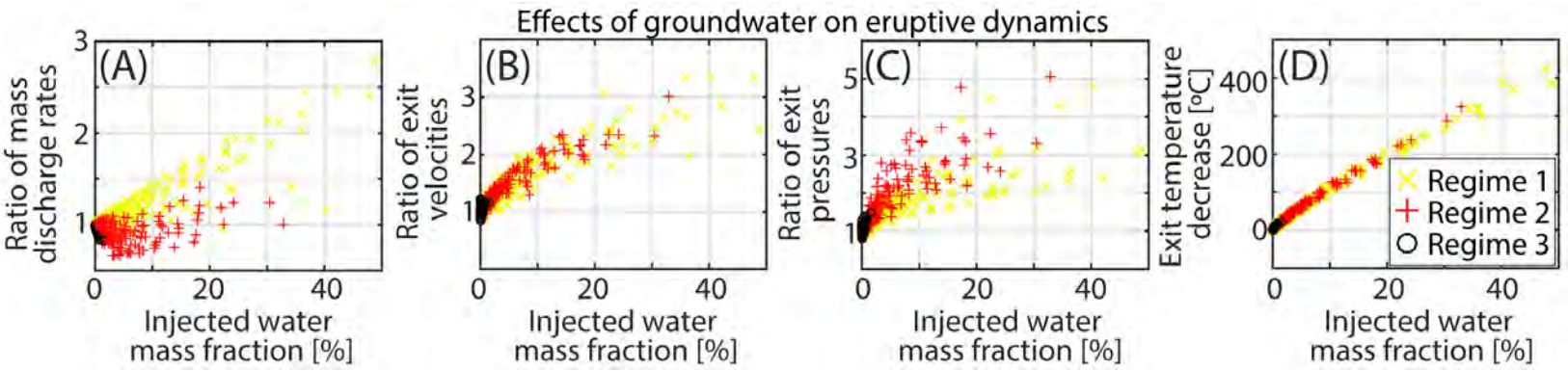
Effects of groundwater on eruptive dynamics
(A)
Ratio of mass discharge rates
Injected water mass fraction [%]
(B)
Ratio of exit velocities
Injected water mass fraction [%]
(C)
Ratio of exit pressures
Injected water mass fraction [%]
(D)
Exit temperature decrease [°C]
Injected water mass fraction [%]
Regime 1
Regime 2
Regime 3